Revisiting Dissolved Organic Matter Analysis using High Resolution Trapped Ion Mobility and FT-ICR Mass Spectrometry

Pablo R. B. Oliveira^{a,b}, Dennys Leyva^{a,b}, Lilian V. Tose^{a,b}, Chad Weisbrod^c, Anton N. Kozhinov^d, Konstantin O. Nagornov^d, Yury O. Tsybin^d and Francisco Fernandez-Lima^{a,b*}

^aDepartment of Chemistry and Biochemistry, Florida International University, Miami, Florida 33199, USA

^bInstitute of Environment, Florida International University, Miami, Florida 33199, USA

^cNational High Magnetic Field Laboratory, Ion Cyclotron Resonance Facility, Florida State University, Tallahassee, Florida 32310-4005, USA

^dSpectroswiss, EPFL Innovation Park, Building 1, 1015 Lausanne, Switzerland

ABSTRACT:

The molecular level characterization of complex mixtures remains an analytical challenge. We have shown that the integration of complementary, high resolution, gas-phase separations allow for chemical formula level isomeric content description. In the current work, we revisited the current challenges associated with the analysis of dissolved organic matter using high resolution trapped ion mobility separation (TIMS) and Fourier transform ion cyclotron resonance mass spectrometry (FT-ICR MS). In particular, we evaluate the separation capabilities provided by TIMS-MS compared to MS alone, the use of ICR complementary data acquisition (DAQ) systems and transient processing strategies, ICR cell geometries (e.g., Infinity cell vs harmonized cell), magnetic field strengths (7 T vs 9.4 T vs 21 T) for the case of a Harney River DOM sample. Results showed that the external high-performance DAQ enables direct representation of mass spectra in the absorption mode FT (aFT), doubling the MS resolution compared to the default magnitude mode FT (mFT). Changes between half- vs full- apodization results in greater MS signal/noise vs superior MS resolving power (RP); in the case of DOM analysis, a 45% increase in assigned formulas is observed when employing the DAQ half (Kaiser-type) apodization window and aFT when compared to the default instrument mFT. Results showed the advantages of reprocessing 2D-TIMS-FT-ICR MS data with higher RP and magnetic field chemical formulae generated list acquired (e.g., 21 T led to a 24% increase in isomers reported) or the implementation of alternative strategies.

INTRODUCTION

Understanding of the chemical composition of complex mixtures in the environment is crucial to uncover their influence on climate change and the global carbon cycle. A common target in environmental analysis is the dissolved organic matter (DOM)—a blend of diverse organic compounds^{1, 2}—which plays a central role in the carbon cycle.^{3, 4} Chemical formula based molecular characterization of DOM has been traditionally done using Ultra-High Resolution Mass Spectrometry (UHR MS) using FT-ICR MS platforms. The UHR capabilities are uniquely provided by Fourier transform ion cyclotron resonance mass spectrometers, FT-ICR MS. The performance metrics of FT ICR-MS, such as resolving power (RP) and acquisition rate, scale linearly with magnetic field strength.⁵ The FT-ICR MS are routinely capable of ultra-high resolution (typically achieving RP > 400 k at m/z 400)⁶⁻⁸ and values of mass measurement accuracy < 1 ppm.⁹ These specifications lend high confidence to the identification of analytes via database search or de novo chemical molecular formula assignment. UHR FT-ICR MS has shown potential to

resolve components from complex mixtures and identify the elemental composition based on accurate mass measurements and relative isotopic ratios at the required RP. ¹⁰⁻¹³ The two flagship FT-ICR systems (one at PNNL and one at NHMFL) employ 21 T magnets that are reaching the limits of state-of-the-art superconducting magnet technology with the required magnetic field characteristics. ^{14, 15}

We have previously described the advantages of complementary ion mobility spectrometry (IMS) and UHR MS for the analysis of complex mixtures. IMS provides insights into ion size and shape through the collision cross section (CCS), which gauges momentum exchange during ion-neutral interactions. ¹⁶⁻¹⁹ In particular, the integration of Trapped IMS (TIMS) with UHR-MS has revealed promising capabilities for swift gas-phase separation, identification, and elucidation of molecular structures; ^{20, 21} noteworthy is that TIMS-MS systematically reduces chemical signal interference. ²²⁻³⁵

Contemporary applications of IMS-UHR MS utilize time-of-flight mass analyzers. However, given the

intricate chemical diversity and complexity of DOM samples, the utilization of FT-ICR MS is essential for accurate chemical formula identification. For example, we previously demonstrated that selected accumulation (SA) TIMS-FT-ICR MS enables target identification through high-resolution mobility and UHR MS analysis of endocrine disruptors in a complex DOM matrix.³⁶ Moreover, the later implementation of oversampling selected accumulation (OSA) TIMS-FT-ICR MS showed an augmented capability for unsupervised feature detection, leveraging high mobility resolving powers $(RP_{IMS} \sim 250)$, along with high mass accuracy (< 1 ppm), and ultrahigh mass resolution (RP of 1.2 M at m/z 400) in a single analysis.²⁶ More recently we showed the TIMS-FT-ICR MS/MS for chemical formula based mobility and MS/MS analysis from a DOM sample and theoretical workflows for structural assignment when standards are not available.³⁷ These results emphasize the imperative need for high resolution mobility separations (RP_{IMS} > 150) combined with UHR-MS to address the structural intricacies inherent in DOM. Higher resolution UHR-MS strategies using FT-ICR MS require longer time-domain transients. Consequently, there is a pressing need to enhance the throughput of FT-ICR MS systems to better synchronize ion detection duty cycles with analyte separation and fractionation processes. Such advancements hold the potential to profoundly impact capabilities by concurrently boosting throughput and resolution, thereby augmenting sensitivity levels.

In this study, we revisit the current challenges of DOM analysis using high resolution TIMS-FT-ICR MS and UHR-MS using cutting-edge data acquisition (DAQ) systems across different ICR cells (e.g., Infinity cell vs harmonized cell) and magnet strengths (7 T vs 9.4 T vs 21 T). The evaluated high-performance DAQ system enables direct representation of mass spectra in the absorption mode FT (aFT), potentially doubling MS resolution compared to the current magnitude mode FT (mFT).³⁸ In addition, differences in peak assignments along the dynamic range observed are described for all platforms.

EXPERIMENTAL SECTION

DOM sample preparation: The DOM sample was collected at the marsh location of the Harney River, Everglades National Park (HR1), at the end of the subtropical winter (April-May 2021). During the collection, a Yellow Springs Instruments (YSI) sensor was used to measure the salinity on site (YSI, Yellow Spring, OH, USA). The sample was obtained at a depth of 50 cm below the surface and stored in 2 L amber plastic bottles (Nalgene, Whaltham, MA, USA) pre-

washed with hydrochloric acid (HCl). Sample was conserved on ice during transportation and stored at 4° C before the solid phase extraction (SPE). The SPE procedure was described elsewhere³⁹⁻⁴¹, but shortly, one liter of sample was acidified with HCl to a pH of 2, then loaded into a 1g-Bond Elut Priority PolLutant (PPL) cartridge (Agilent, Santa Clara, CA, USA). The PPL cartridge was preconditioned with one-cartridge volume of methanol, and two-cartridges volume of water (pH 2). After the sample was loaded, the cartridge was rinsed with water (pH 2) and dried with nitrogen gas for 5 minutes preceding the elution with 20 mL of methanol. Finally, the SPE with methanol was stored in prewashed glass vials at - 20° C. All solvents used were Optima LC-MS grade obtained from Fisher Scientific (Pittsburgh, PA, USA).

7 T TIMS-FT-ICR MS: DOM HR-1 samples were diluted to a final concentration of ~10 ppm in a 1:9 methanol:ethanol v:v solution. The custom-built Solarix 7 T TIMS-FT-ICR MS setup has been described in detail elsewhere. 8, 26, 42, 43 Briefly, a custom-built TIMS cell replace the default ion funnel cartridge and was operated using LabVIEW (National Instruments) software synchronized with the FTMS control acquisition program (Bruker Daltonics); the commercial 7 T FT-ICR MS was fitted with an ICR infinity cell. An electrospray ionization (ESI) source (Apollo II ESI design, Bruker Daltonics, MA) was used. Common operating parameters were a TIMS funnel radio frequency (rf) amplitude of 220 peak-to-peak voltage (V_{pp}) at 1240 kHz; capillary exit – 100 V; deflector plate with - 90 V; skimmer1 voltage of - 15 V; octopole rf amplitude of 350 V_{pp}; and a rf of 1000 V_{pp} for the collision cell. The TIMS was operated in OSA mode (see details in Figure 1). In a sequence of 150 pulses, a non-linear scan ramp from 10-110 V was used, with a 4 V analytical component and 0.2 V across the steps. The TIMS gate was pulsed at the end of the analytical ramp component using a - 6 to 30 V pulse. Multiple TIMS scans were performed per ICR MS scan. Nitrogen gas was used as a bath gas at 300 K, and the velocity of the gas was defined by the pressure difference across the TIMS funnel 2.4 mbar to 1.0 mbar. The experimental data was processed using the Peak-by-Peak software (Spectroswiss, Lausanne, Switzerland) and summarized in a MS peak list corresponding to the mFT Solarix ICR Infinity cell acquisition (7T-I-mFT).

9.4 T ESI-FT-ICR MS: A SolariX 9.4 T FT-ICR MS (Bruker Daltonics, MA) equipped with a harmonized ICR cell (ParaCell) was used. DOM HR-1 samples were diluted to a final concentration of ~ 5 ppm in a 1:20 methanol:ethanol v:v solution. The diluted DOM

sample was ionized using a nano ESI (nESI) emitter in negative ion mode. These pulled tips were produced from quartz capillaries (O.D. = 1.0 mm and I.D. = 0.70mm) employing a Sutter Instruments Co. P2000 laser puller (Sutter Instruments, CA). In those the DOM solution was loaded together with a tungsten wire biased at ~ 900 V relative to the MS inlet. Common operating parameters were a funnel radio frequency (rf) amplitude of 100 V_{pp} at 1240 kHz; capillary exit of - 100 V; deflector plate width – 120 V; skimmer1 voltage of – 15 V; octopole rf amplitude of 350 V_{pp}; and a rf of 1000 V_{pp} for the collision cell. ICR time-domain signals (transients) were also captured in parallel using an external high-performance DAQ system (FTMS Booster X3T, Spectroswiss, Lausanne, Switzerland). The experimental data was processed using the Peakby-Peak software (Spectroswiss) and summarized in three MS peak lists corresponding to the mFT Solarix ICR ParaCell (9T-P-mFT), and two absorption modes using half-window Kaiser apodization (9T-P-aFTsk), and full-window Kaiser apodization (9T-P-aFTk) from the DAO system.

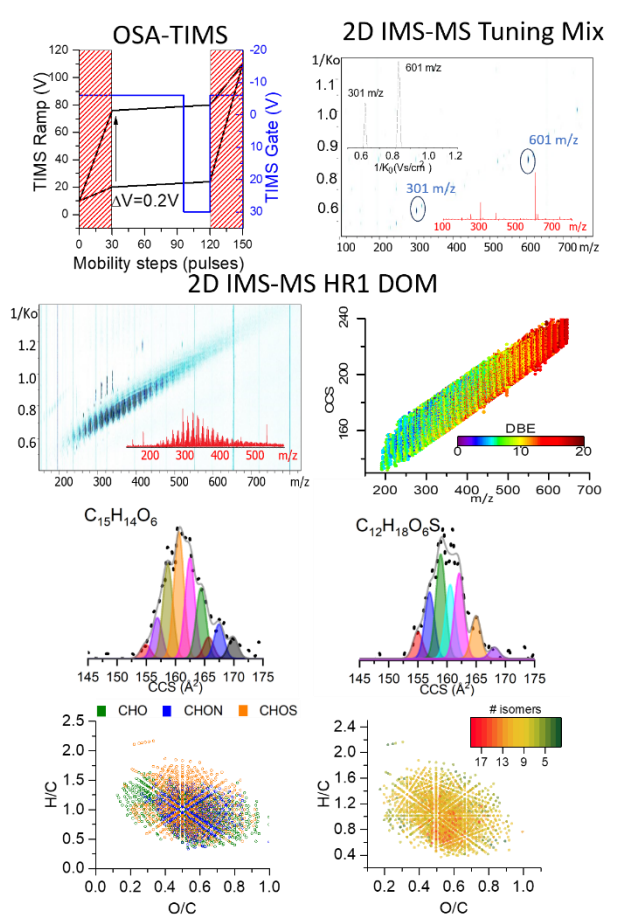


Figure 1. Typical OSA ESI(-) TIMS-FT-ICR MS analysis of a DOM HR-1 using non-linear mobility scan functions. Mobility scans are calibrated using known standards (e.g., Tuning Mix) in a single step

followed by 1D MS peak detection, chemical formula analysis, SAME software processing for isomeric content and visualization using Van Krevelen plots including the isomeric content.

21 T ESI-FT-ICR MS: Details about the 21 T FT-ICR MS from the National High Magnetic Field Laboratory (NHMFL, Tallahassee, FL) can be found elsewhere. Heiefly, DOM HR-1 samples were infused at 100 ppm using an ESI source. 1 x 106 ions (charges) were accumulated and analyzed, with 100 time-domain acquisitions averaged for all experiments. Ion mobility measurements were not conducted in this setup. The experimental data was processed using the Peak-by-Peak software (Spectroswiss) and summarized in a MS peak list corresponding to the magnitude mode ICR ParaCell cell acquisition (21T-p-mFT)

MS data processing: Composer software (v. 1.0.6, Sierra Analytics, Modesto, CA) was used for chemical formula assignment from the MS peak lists. Formula assignments were performed using the DOM theoretical constraints: $C_{4-50}H_{4-100}N_{0-3}O_{0-25}S_{0-2}$, S/N > 3, m/z range 100-650, error < 1 ppm and 0 < O/C < 1, 0.3 < H/C < 2.5, and double bond equivalent minus oxygen (DBE-O) < 10.45

The peak signal was measured from the zero level across all datasets, whereas the noise was assessed by determining the range of baseline noise from its minimum to maximum values. The MS RP was calculated as the ratio of the peak position in a mass spectrum (m/z) and the full width at half maximum of this peak $(\Delta m/z_{50\%})$,

$$RP = \frac{m/z}{\Delta m/z_{50\%}} \quad (1)$$

TIMS data processing. An Agilent Tuning Mix calibration standard was used for the ion mobility calibration (see Figure 1 for typical 2D-IMS MS and IMS and MS projections).46 A custom-build Software Assisted Molecular Elucidation (SAME) written in Python (v 3.7.3) was used to estimate the number of isomers per chemical formula. The SAME program uses noise removal, mean gap filling, asymmetric least squares smoothing for base line correction, continuous wavelet transform (CWT)-based peak detection (SciPy package) and Gaussian fitting with non-linear least squares functions (Levenberg-Marquardt algorithm).⁴² 2D-IMS-MS data were processed using the peak lists from the 7T-I-mFT and 21T-P-mFT datasets to evaluate the influence of the chemical noise during 1D-MS processing of the IMS-MS data. Graphs were generated using OriginPro 2016 (OriginLab, Northamption, MA) and Microsoft Excel 365.

RESULTS AND DISCUSSION

Advantages of complementary TIMS and FT-ICR MS for the analysis of DOM: A typical 2D TIMS-MS contour plots of an ESI(-)-TIMS-FT-ICR MS analysis of DOM results on a single trend line, mostly composed of singly charge species (Figure 1). The MS projection, sum of all mass spectra obtained across different mobilities, shows a gaussian like distribution centered around 350 m/z, with a typical even odd periodicity. When mobility calibrated and SAME processed, each mobility profile at the level of chemical formula can be segmented by the minimal number of potential isomers (up to 18 isomers per formula were observed, represented by different peak colors). As the m/z increases, an increase in the CCS and double bond equivalent (DBE) number are observed, suggesting an increase in structural complexity. Different from traditional analysis, Van Krevelen (VK) plots can be enhanced with the isomeric content, as a better reflection of the structural composition of the sample.⁴⁷ This approach complements the elemental composition data shown in the left VK plot, offering a more complete picture of the sample's molecular characteristics. Nevertheless, this procedure is biased by the peak list and chemical formula assignment from the 1D MS processing; that is, current approaches do not take advantage of the potential 2D IMS-MS feature detection.

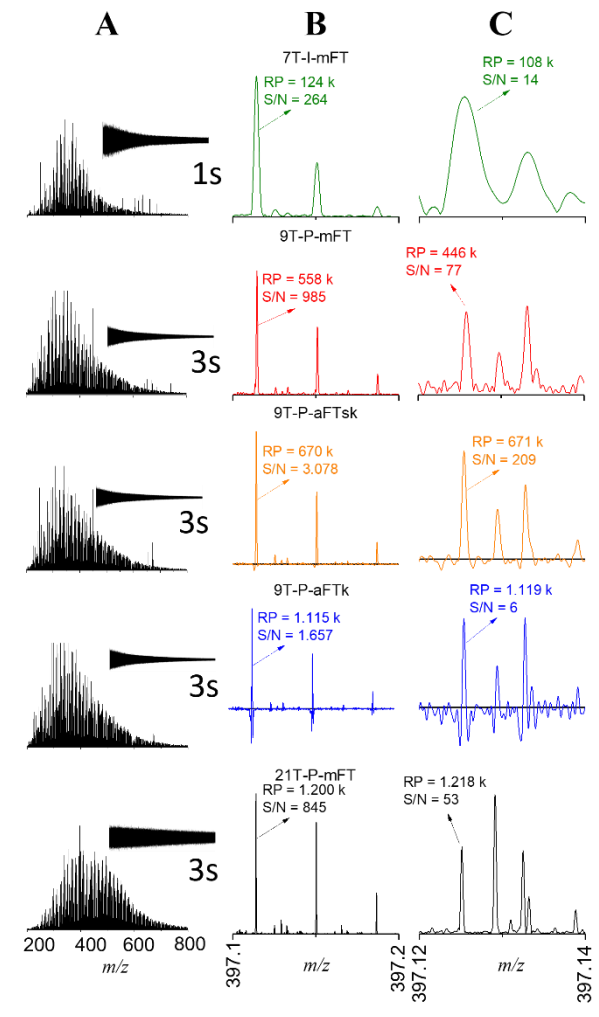


Figure 2. Typical ESI(-) FT-ICR MS mass spectra of DOM HR-1 as a function of the ICR cell type, magnetic field strength and transient processing. (A) Broadband FT-ICR mass spectra and transient time for each experiment. MS segments 397.1-397.2 (B) and 397.12-397.14 (C) m/z.

Influence of ICR cell, magnetic field, and ICR transient processing: A typical broadband, ESI(-) FT-ICR MS spectra of DOM HR-1 are shown in Figure 2 for a 7 T (7T-I-mFT), 9.4 T (9T-P-mFT, 9T-P-aFTsk and 9T-P-aFTk), and 21 T (21T-P-mFT) magnets, configurations, and transient processing modes. Inspection of Figure 2 shows a similar gaussian like distribution spanning across m/z 200-800. The center of the distribution and the transient (or a free induction decay, FID) varies slightly with the magnetic field, the higher the magnetic field the higher is the center of the distribution, longer the transient and smaller the FID dampening.

Processing of the transients (FID) showed changes in the MS RP and the signal-to-noise ratio (S/N) across the

configurations (m/z 397.10 - 397.2 and m/z 397.12 -397.14 in Figure 2 B and C). As expected, the RP scales with the magnetic field as well as the differences between magnitude and absorption mode ($\sim 2x$). With respect to the FID processing using different Kaiser apodization forms, a discernible contrast emerges between the half (9T-P-aFTsk) and full (9T-P-aFTk) window apodization methods: half aFTsk provides greater MS S/N, while full aFTk provides superior MS RP. As the m/z increases, there is a discernible escalation in the requirement for higher RP to effectively discern compounds at the nominal mass level and subsequently the number of chemical formulae assigned. For example, at the nominal mass m/z 397, an increase from 19 (7T-I-mFT) to 86 (21T-PmFT) formulas is observed (Figure S1, Supporting Information).

The net effect of RP and S/N can be better evaluated by the comparison of the number of peaks detected and the chemical formulas assigned (Figure 3). Since the same criteria and software were used, differences in assignments can be correlated back to the quality of the mass spectra under the discussed conditions (Figure 2). Inspection of Figure 3 shows a poor assignment of chemical formulas when compared to the total number of peaks detected, regardless of the configuration considered and the dynamic range; that is, high S/N resolved peaks remain unidentified. While some of it can be related to the heteroatom list, isotopes considered, as well as structural constraints imposed during the assignment, it remains a point for further evaluation during DOM analysis.

Differences between the chemical formula assigned and their correlation with the DOM structural composition can be observed in the VK diagrams (Figure 3 B). The representation of elemental ratios within this compositional framework reveals a cluster of fundamental molecules situated within the lignin-like region (0.5 < H/C < 1.4 and 0.3 < O/C < 0.7) of the VK diagram. This cluster increases in density with higher MS RP and magnetic field strength.

A closer examination of the dynamic range for individual classes within each dataset (Fig. S2), reveals that the CHO class serves as the primary contributor to the spectra abundance, whereas the CHON class represents formulas with the least abundance.

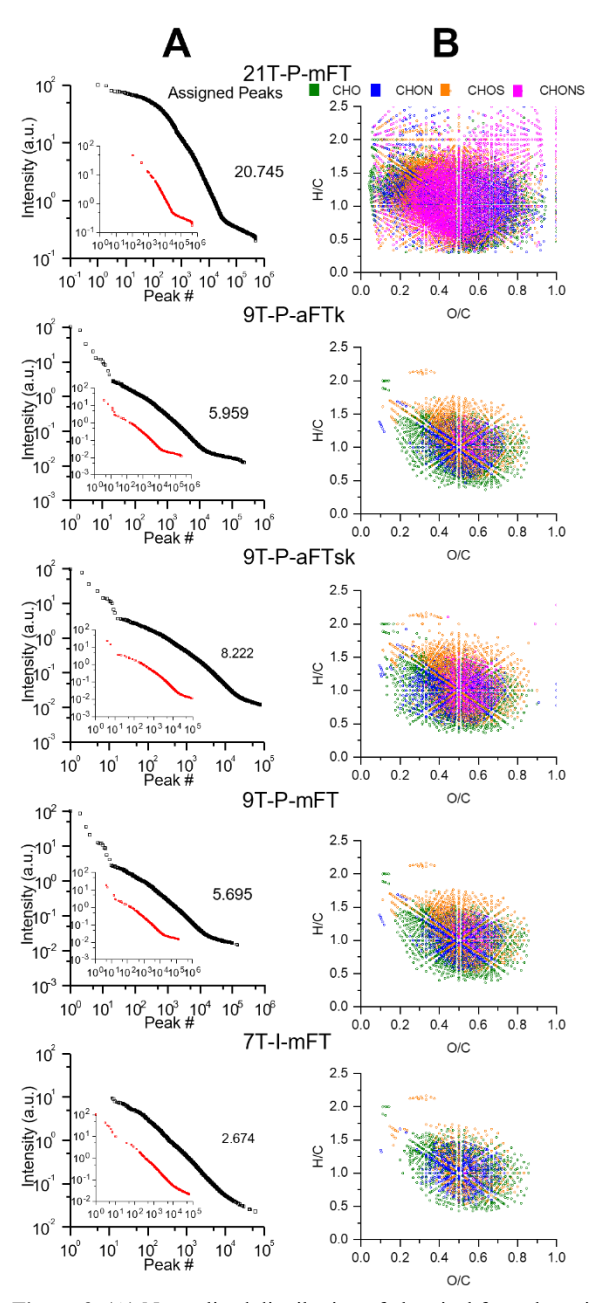


Figure 3. (A) Normalized distribution of chemical formula assigned (black), not assigned peaks (red inset) and (B) corresponding Van Krevelen plots as a function of the ICR cell type, magnetic field strength, and FID (transient) processing.

Inspection of the lowest abundant heteroatom series provides further insight across the modes described. For example, the number of assigned formulas in the CHONS class exhibits a considerable change with the magnetic field (4,040 and 16 formulas using 21T-P-mFT and 7T-I-mFT, respectively). Previous work using 7 T systems did not report this series during DOM ESI(-) analysis.⁴⁷ Despite this variance in contribution, the separation per heteroatom class showcases different

distributions across the dynamic range. Members from all classes are detected even among the least abundant peaks.

A breakdown of chemical formula assigned relative to the peak lists and across platforms is summarized in Figure 4. Only 3 - 7% of the peaks determined with a 3 σ noise threshold were correlated to a chemical formula. A near linear increase in the number of assigned chemical formulas is observed with the increase in the magnetic field (from 7 T to 21 T). When data are acquired at the same field (9T-P-aFTsk vs 9T-P-mFT), a 45% increase in assigned formulas observed when employing the DAQ half apodization window and absorption mode when compared to the default magnitude mode.

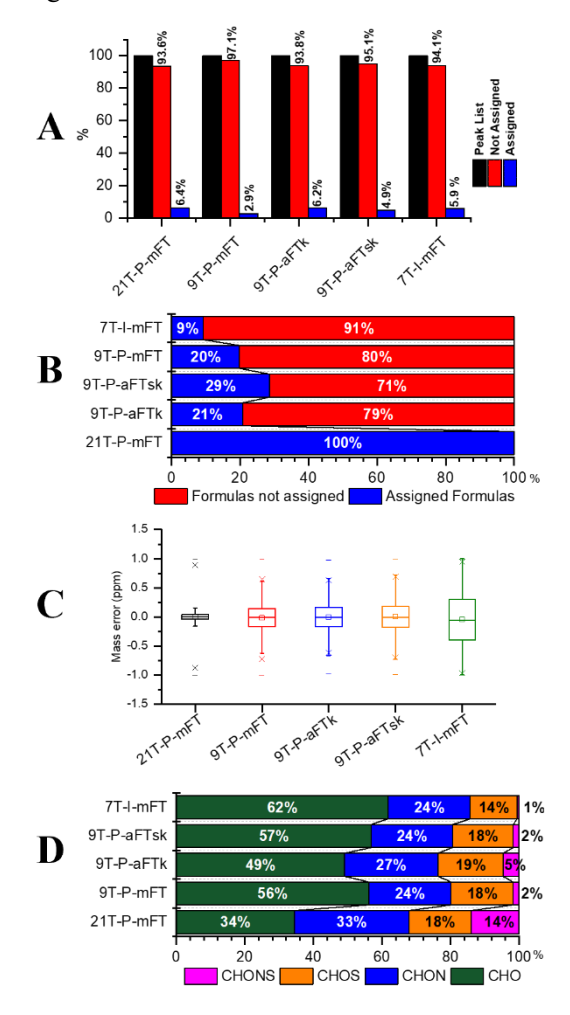


Figure 4. Summary of chemical formulas assigned relative to the total number of peaks (A) and to the 21 T peak list (B), mass errors (C) and distribution by heteroatom class (D) as a function of the ICR cell type, magnetic field strength and FID (transient) processing.

The chemical formula assignment mass error follows the expected trend: as the magnetic field increases, there is an increase in the mass accuracy (Figure 4 C). The chemical formula error assignment increases with the m/z (Fig. S3). The comparison across the 9 T datasets shows no significant differences in mass error

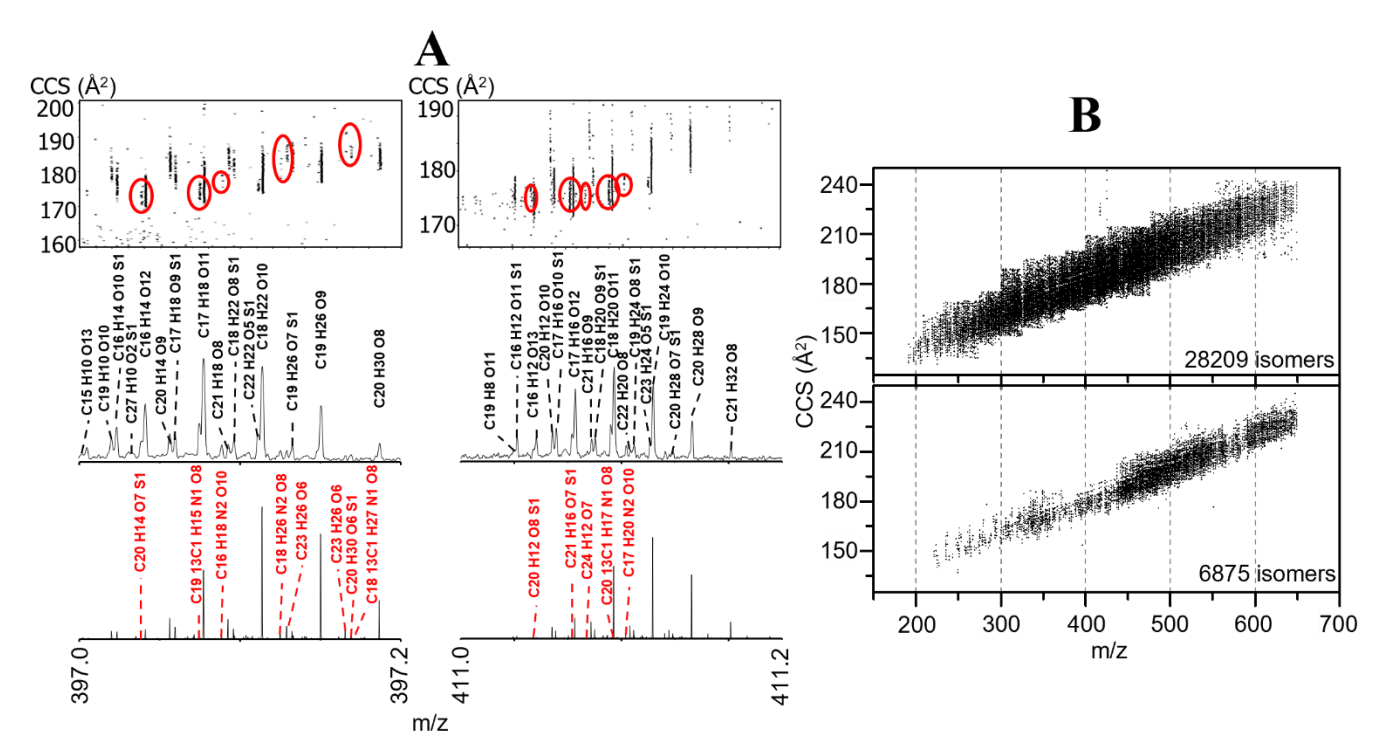


Figure 5. (A) DOM HR-1 2D TIMS-MS contour plot and corresponding 7 T and 21 T MS projections at m/z 397 and 411 nominal mass. Red circles correspond to newly detected formulas and isomers using the 21 T list. (B) Represents the distribution of isomers as a function of the m/z using the 7 T list (top) and new isomers detected with the 21 T list (bottom).

distribution (< 25 ppb), despite the differences in number of chemical formulas assigned between them.

Influence of 1D MS processing for the 2D-IMS-MS isomeric content analysis. A comparison of the 2D TIMS-MS dataset processing using the 7 T and 21 T chemical formula list is shown in Figure 5. Closer inspection at nominal mass shows the challenges associated with the 1D MS processing (m/z 397 and 411 nominal mass). Chemical formulas associated to the signals detected with the 7 T MS experiment are depicted in black. Moreover, several signals observed in the 2D IMS-MS plot were not resolved in the 7 T MS experiment but are in the 21 T MS experiment, as indicated by the red circles in Figure 5. When the 2D-IMS-MS dataset is reprocessed using the 21 T MS list, the number of changes from 28209 to 35084. Most of the new detected isomers are in the m/z 450-650 range (Figure 5 B). Nevertheless, new peaks were observed across the entire distribution.

CONCLUSIONS:

Challenges associated with the analysis of complex mixtures, with emphasis on dissolved organic matter (DOM) isomeric complexity were described. in particular, we showed the advantages of ESI(-)TIMS-

FT-ICR MS to dissect the chemical complexity at the molecular level and isomeric level. Moreover, challenges associated to the ICR cell geometry, magnetic field and modes of acquistion and processing were described.

With the magnetic field increase, a natural increase in dynamic range and mass accuracy lead to a higher number of chemical formulas detected. Moreover, changes between magnitude mode and absorption mode, as well as half vs full window apodization of the FID signal lead to significant differences in chemical formula assignments (~ 45%). This work also showcases that challenges in the chemical formula assignment are not necessarily associated to the dynamic range or mass resolution, since a good portion of the not assigned formulas were not from the lower part of the dynamic range distribution.

Most importantly, it was shown the advantages of reprocessing 2D-IMS-FT-ICR MS data with 1D MS chemical fomula list acquired at 21 T (24% increase in isomers reported) or the implementation of alternative strategies. Given the low number of 21 T instruments, future research should evaluate the integration of 2D processing algorithms based on DAQ system acquired transients and mass spectra, and the utilization of the

high-performance DAQ-enhanced RP and signal-tonoise ratio when applied to a conventional FT-ICR MS system.

ASSOCIATED CONTENT

Supporting Information

The Supporting Information is available free of charge at http://pubs.acs.org. Figure S1, comparison between assigned formulas at m/z 397 for each dataset; Figure S2, dynamic range of assigned chemical formulas, segregated by class for each dataset, demonstrating distinct distribution patterns for each class; Figure S3, elemental compositions assigned for each dataset, plotted based on mass error versus m/z, accompanied by RMS error and standard deviation.

AUTHOR INFORMATION

Corresponding Author

Francisco Fernandez-Lima — Department of Chemistry and Biochemistry, Biomolecular Science Institute, Florida International University, Miami, Florida 33199, USA; orcid.org/0000-0002-1283-4390; Email: fernandf@fiu.edu

Author

Pablo R. B. Oliveira — Department of Chemistry and Biochemistry, Florida International University, Miami, Florida 33199, United States.

Lilian V. Tose – Department of Chemistry and Biochemistry, Florida International University, Miami, Florida 33199, United States.

Dennys Leyva — Department of Chemistry and Biochemistry, Florida International University, Miami, Florida 33199, USA.

Chad Weisbrod – National High Magnetic Field Laboratory, Ion Cyclotron Resonance Facility, Florida State University, Tallahassee, Florida 32310-4005, United States.

Anton N. Kozhinov – Spectroswiss, EPFL Innovation Park, Building I, 1015 Lausanne, Switzerland.

Konstantin O. Nagornov – Spectroswiss, EPFL Innovation Park, Building I, 1015 Lausanne, Switzerland.

Yury O. Tsybin – Spectroswiss, EPFL Innovation Park, Building I, 1015 Lausanne, Switzerland.

Notes

ANK, KON, and YOT are employees of Spectroswiss, a company that develops hardware and software for data acquisition, processing, and analysis for mass spectrometry. Other authors declare no competing financial interest.

ACKNOWLEDGEMENTS

This work was supported by the NSF CHEM 2304837. D.L. acknowledges the fellowship provided by the National Science Foundation award (HRD-1547798) to Florida International University as part of the Centers for Research Excellence in Science and Technology (CREST) Program. D.L. also would

like to acknowledge John Kominoski, Edward Castañeda, Ryan Bremen, and Kenny Anderson from the Ecosystem Ecology Laboratory at Florida International University (FIU) for their field and laboratory support. This is contribution number 1768 from the Institute of Environment at Florida International University. This material was developed in collaboration with the Florida Coastal Everglades Long Term Ecological Research program under the National Science Foundation Grant No. DEB-2025954. The authors acknowledge the personnel of the Advance Mass Spectrometry Facility at Florida International University as well as David Stranz and Sierra Analytics, Inc. for their support with the Composer software.

REFERENCES

- (1) Keenan, T. F.; Williams, C. A. The Terrestrial Carbon Sink. *Annual Review of Environment and Resources* **2018**, *43* (1), 219-243. DOI: 10.1146/annurev-environ-102017-030204.
- (2) Hedges, J. I. Global biogeochemical cycles: progress and problems. *Marine Chemistry* **1992**, *39* (1), 67-93. DOI: https://doi.org/10.1016/0304-4203(92)90096-S.
- (3) Buchan, A.; LeCleir, G. R.; Gulvik, C. A.; González, J. M. Master recyclers: features and functions of bacteria associated with phytoplankton blooms. *Nature Reviews Microbiology* **2014**, *12* (10), 686-698. DOI: 10.1038/nrmicro3326.
- (4) Moeckel, C.; Monteith, D. T.; Llewellyn, N. R.; Henrys, P. A.; Pereira, M. G. Relationship between the Concentrations of Dissolved Organic Matter and Polycyclic Aromatic Hydrocarbons in a Typical U.K. Upland Stream. *Environmental Science & Technology* **2014**, *48* (1), 130-138. DOI: 10.1021/es403707q. (5) Marshall, A. G.; Guan, S. Advantages of High Magnetic Field for Fourier Transform Ion Cyclotron Resonance Mass Spectrometry. *Rapid Communications in Mass*

https://doi.org/10.1002/(SICI)1097-

Spectrometry 1996, 10 (14), 1819-1823. DOI:

- 0231(199611)10:14
 (6) Benigni, P.; Bravo, C.; Quirke, J. M. E.; DeBord, J. D.; Mebel, A. M.; Fernandez-Lima, F. Analysis of Geologically Relevant Metal Porphyrins Using Trapped Ion Mobility Spectrometry–Mass Spectrometry and Theoretical
- Spectrometry–Mass Spectrometry and Theoretical Calculations. *Energy & Fuels* **2016**, *30* (12), 10341-10347. DOI: 10.1021/acs.energyfuels.6b02388.
- (7) Benigni, P.; Sandoval, K.; Thompson, C. J.; Ridgeway, M. E.; Park, M. A.; Gardinali, P.; Fernandez-Lima, F. Analysis of Photoirradiated Water Accommodated Fractions of Crude Oils Using Tandem TIMS and FT-ICR MS. *Environ Sci Technol* **2017**, *51* (11), 5978-5988. DOI: 10.1021/acs.est.7b00508 From NLM Medline.
- (8) Tose, L. V.; Benigni, P.; Leyva, D.; Sundberg, A.; Ramírez, C. E.; Ridgeway, M. E.; Park, M. A.; Romão, W.; Jaffé, R.; Fernandez-Lima, F. Coupling trapped ion

- mobility spectrometry to mass spectrometry: trapped ion mobility spectrometry—time-of-flight mass spectrometry versus trapped ion mobility spectrometry—Fourier transform ion cyclotron resonance mass spectrometry. *Rapid Communications in Mass Spectrometry* **2018**, *32* (15), 1287-1295. DOI: 10.1002/rcm.8165.
- (9) Kujawinski, E. B.; Del Vecchio, R.; Blough, N. V.; Klein, G. C.; Marshall, A. G. Probing molecular-level transformations of dissolved organic matter: insights on photochemical degradation and protozoan modification of DOM from electrospray ionization Fourier transform ion cyclotron resonance mass spectrometry. *Marine Chemistry* **2004**, *92* (1-4), 23-37. DOI: 10.1016/j.marchem.2004.06.038.
- (10) McKenna, A. M.; Williams, J. T.; Putman, J. C.; Aeppli, C.; Reddy, C. M.; Valentine, D. L.; Lemkau, K. L.; Kellermann, M. Y.; Savory, J. J.; Kaiser, N. K.; et al. Unprecedented Ultrahigh Resolution FT-ICR Mass Spectrometry and Parts-Per-Billion Mass Accuracy Enable Direct Characterization of Nickel and Vanadyl Porphyrins in Petroleum from Natural Seeps. *Energy & Fuels* **2014**, *28* (4), 2454-2464. DOI: 10.1021/ef5002452 (acccessed 2014/10/14).
- (11) Marshall, A. G.; Rodgers, R. P. Petroleomics: The Next Grand Challenge for Chemical Analysis. *Acc. Chem. Res.* **2004**, *37*, 53-59.
- (12) Hughey, C. A.; Rodgers, R. P.; Marshall, A. G. Resolution of 11 000 Compositionally Distinct Components in a Single Electrospray Ionization Fourier Transform Ion Cyclotron Resonance Mass Spectrum of Crude Oil. Analytical Chemistry 2002, 74 (16), 4145-4149. DOI: 10.1021/ac020146b (acccessed 2014/05/21). (13) Qian, K.; Rodgers, R. P.; Hendrickson, C. L.; Emmett, M. R.; Marshall, A. G. Energy Fuels 2001, 15, 492. (14) Hendrickson, C. L.; Quinn, J. P.; Kaiser, N. K.; Smith, D. F.; Blakney, G. T.; Chen, T.; Marshall, A. G.; Weisbrod, C. R.; Beu, S. C. 21 Tesla Fourier Transform Ion Cyclotron Resonance Mass Spectrometer: A National Resource for Ultrahigh Resolution Mass Analysis. Journal of the American Society for Mass Spectrometry 2015, 26 (9), 1626-1632, journal article. DOI: 10.1007/s13361-015-1182-2.
- (15) Shaw, J. B.; Lin, T.-Y.; Leach III, F. E.; Tolmachev, A. V.; Tolić, N.; Robinson, E. W.; Koppenaal, D. W.; Paša-Tolić, L. 21 Tesla Fourier transform ion cyclotron resonance mass spectrometer greatly expands mass spectrometry toolbox. *Journal of The American Society for Mass Spectrometry* **2016**, *27* (12), 1929-1936. (16) McDaniel, E. W.; Mason, E. A. *Mobility and diffusion of ions in gases*; John Wiley and Sons, Inc., New York, 1973.

- (17) Kanu, A. B.; Dwivedi, P.; Tam, M.; Matz, L.; Hill, H. H. Ion mobility-mass spectrometry. Journal of Mass Spectrometry 2008, 43 (1), 1-22. DOI: 10.1002/jms.1383. (18) Maurer, M. M.; Donohoe, G. C.; Valentine, S. J. Advances in ion mobility-mass spectrometry instrumentation and techniques for characterizing structural heterogeneity. Analyst 2015, 140, 6782-6798, 10.1039/C5AN00922G. DOI: 10.1039/c5an00922g. (19) Wyttenbach, T.; Pierson, N. A.; Clemmer, D. E.; Bowers, M. T. Ion Mobility Analysis of Molecular Dynamics. *Annu Rev Phys Chem* **2014**, *65*, 175-196. DOI: DOI 10.1146/annurev-physchem-040513-103644. (20) Fernandez-Lima, F. A.; Kaplan, D. A.; Suetering, J.; Park, M. A. Gas-phase separation using a Trapped Ion Mobility Spectrometer. International Journal for Ion Mobility Spectrometry 2011, 14 (2-3), 93-98. (21) Fernandez-Lima, F. A.; Kaplan, D. A.; Park, M. A. Note: Integration of trapped ion mobility spectrometry with mass spectrometry. Rev. Sci. Instr. 2011, 82 (12), 126106.
- (22) Castellanos, A.; Benigni, P.; Hernandez, D. R.; DeBord, J. D.; Ridgeway, M. E.; Park, M. A.; Fernandez-Lima, F. A. Fast Screening of Polycyclic Aromatic Hydrocarbons using Trapped Ion Mobility Spectrometry Mass Spectrometry. *Anal. Meth.* **2014**, *6*, 9328-9332. (23) Benigni, P.; Thompson, C. J.; Ridgeway, M. E.; Park, M. A.; Fernandez-Lima, F. Targeted High-Resolution Ion Mobility Separation Coupled to Ultrahigh-Resolution Mass Spectrometry of Endocrine Disruptors in Complex Mixtures. *Anal. Chem.* **2015**, *87* (8), 4321-4325. DOI: 10.1021/ac504866v.
- (24) Hernandez, D. R.; DeBord, J. D.; Ridgeway, M. E.; Kaplan, D. A.; Park, M. A.; Fernandez-Lima, F. A. Ion dynamics in a trapped ion mobility spectrometer. *Analyst* **2014**, *139* (8), 1913-1921, 10.1039/C3AN02174B. DOI: 10.1039/C3AN02174B.
- (25) Adams, K. J.; Montero, D.; Aga, D.; Fernandez-Lima, F. Isomer separation of polybrominated diphenyl ether metabolites using nanoESI-TIMS-MS. International Journal for Ion Mobility Spectrometry 2016, 1-8, journal article. DOI: 10.1007/s12127-016-0198-z. (26) Benigni, P.; Fernandez-Lima, F. Oversampling Selective Accumulation Trapped Ion Mobility Spectrometry Coupled to FT-ICR MS: Fundamentals and Applications. Analytical Chemistry 2016, 88 (14), 7404-7412. DOI: 10.1021/acs.analchem.6b01946. (27) Benigni, P.; Marin, R.; Molano-Arevalo, J. C.; Garabedian, A.; Wolff, J. J.; Ridgeway, M. E.; Park, M. A.; Fernandez-Lima, F. Towards the analysis of high molecular weight proteins and protein complexes using TIMS-MS. International Journal for Ion Mobility Spectrometry 2016, 1-10, journal article. DOI: 10.1007/s12127-016-0201-8.

(28) Silveira, J. A.; Ridgeway, M. E.; Laukien, F. H.; Mann, M.; Park, M. A. Parallel accumulation for 100% duty cycle trapped ion mobility-mass spectrometry. *International Journal of Mass Spectrometry*. DOI:

http://dx.doi.org/10.1016/j.ijms.2016.03.004.

- (29) Michelmann, K.; Silveira, J. A.; Ridgeway, M. E.; Park, M. A. Fundamentals of Trapped Ion Mobility Spectrometry. *Journal of The American Society for Mass Spectrometry* **2015**, *26* (1), 14-24, journal article. DOI: 10.1007/s13361-014-0999-4.
- (30) Silveira, J. A.; Michelmann, K.; Ridgeway, M. E.; Park, M. A. Fundamentals of Trapped Ion Mobility Spectrometry Part II: Fluid Dynamics. *Journal of The American Society for Mass Spectrometry* **2016**, *27* (4), 585-595, journal article. DOI: 10.1007/s13361-015-1310-z.
- (31) Silveira, J. A.; Danielson, W.; Ridgeway, M. E.; Park, M. A. Altering the mobility-time continuum: nonlinear scan functions for targeted high resolution trapped ion mobility-mass spectrometry. *International Journal for Ion Mobility Spectrometry* **2016**, 1-8, journal article. DOI: 10.1007/s12127-016-0196-1.
- (32) Ridgeway, M. E.; Silveira, J. A.; Meier, J. E.; Park, M. A. Microheterogeneity within conformational states of ubiquitin revealed by high resolution trapped ion mobility spectrometry. *Analyst* **2015**, *140* (20), 6964-6972, 10.1039/C5AN00841G. DOI: 10.1039/C5AN00841G.
- (33) Meier, F.; Beck, S.; Grassl, N.; Lubeck, M.; Park, M. A.; Raether, O.; Mann, M. Parallel Accumulation—Serial Fragmentation (PASEF): Multiplying Sequencing Speed and Sensitivity by Synchronized Scans in a Trapped Ion Mobility Device. *Journal of Proteome Research* 2015, 14 (12), 5378-5387. DOI: 10.1021/acs.jproteome.5b00932. (34) Ridgeway, M. E.; Wolff, J. J.; Silveira, J. A.; Lin, C.; Costello, C. E.; Park, M. A. Gated trapped ion mobility spectrometry coupled to fourier transform ion cyclotron resonance mass spectrometry. *International Journal for Ion Mobility Spectrometry* 2016, 1-9, journal article. DOI: 10.1007/s12127-016-0197-0.
- (35) Pu, Y.; Ridgeway, M. E.; Glaskin, R. S.; Park, M. A.; Costello, C. E.; Lin, C. Separation and Identification of Isomeric Glycans by Selected Accumulation-Trapped Ion Mobility Spectrometry-Electron Activated Dissociation Tandem Mass Spectrometry. *Analytical Chemistry* **2016**, *88* (7), 3440-3443. DOI: 10.1021/acs.analchem.6b00041. (36) Benigni, P.; Thompson, C. J.; Ridgeway, M. E.; Park, M. A.; Fernandez-Lima, F. Targeted high-resolution ion mobility separation coupled to ultrahigh-resolution mass spectrometry of endocrine disruptors in complex mixtures. *Analytical Chemistry* **2015**, *87* (8), 4321-4325. DOI: 10.1021/ac504866v.

- (37) Leyva, D.; Jaffe, R.; Fernandez-Lima, F. Structural Characterization of Dissolved Organic Matter at the Chemical Formula Level Using TIMS-FT-ICR MS/MS. *Analytical Chemistry* **2020**, *92* (17), 11960-11966. DOI: 10.1021/acs.analchem.0c02347.
- (38) Nagornov, K. O.; Kozhinov, A. N.; Nicol, E.; Tsybin, O. Y.; Touboul, D.; Brunelle, A.; Tsybin, Y. O. Narrow Aperture Detection Electrodes ICR Cell with Quadrupolar Ion Detection for FT-ICR MS at the Cyclotron Frequency. Journal of the American Society for Mass Spectrometry **2020**, 31 (11), 2258-2269. DOI: 10.1021/jasms.0c00221. (39) Dittmar, T.; Koch, B.; Hertkorn, N.; Kattner, G. A simple and efficient method for the solid-phase extraction of dissolved organic matter (SPE-DOM) from seawater. Limnology and Oceanography: Methods 2008, 6 (6), 230-235. DOI: 10.4319/lom.2008.6.230. (40) Hertkorn, N.; Harir, M.; Cawley, K. M.; Schmitt-Kopplin, P.; Jaffé, R. Molecular characterization of dissolved organic matter from subtropical wetlands: A comparative study through the analysis of optical properties, NMR and FTICR/MS. Biogeosciences 2016, 13 (8), 2257-2277. DOI: 10.5194/bg-13-2257-2016. (41) Li, Y.; Harir, M.; Lucio, M.; Kanawati, B.; Smirnov, K.; Flerus, R.; Koch, B. P.; Schmitt-Kopplin, P.; Hertkorn, N. Proposed Guidelines for Solid Phase Extraction of Suwannee River Dissolved Organic Matter. Analytical Chemistry 2016, 88 (13), 6680-6688. DOI: 10.1021/acs.analchem.5b04501.
- (42) Benigni, P.; Marin, R.; Sandoval, K.; Gardinali, P.; Fernandez-Lima, F. Chemical Analysis of Water-accommodated Fractions of Crude Oil Spills Using TIMS-FT-ICR MS. *Journal of Visualized Experiments* **2017**, (121). DOI: 10.3791/55352.
- (43) Benigni, P.; Porter, J.; Ridgeway, M. E.; Park, M. A.; Fernandez-Lima, F. Increasing Analytical Separation and Duty Cycle with Nonlinear Analytical Mobility Scan Functions in TIMS-FT-ICR MS. *Analytical Chemistry* **2018**, *90* (4), 2446-2450. DOI: 10.1021/acs.analchem.7b04053. (44) Hendrickson, C. L.; Quinn, J. P.; Kaiser, N. K.; Smith, D. F.; Blakney, G. T.; Chen, T.; Marshall, A. G.; Weisbrod, C. R.; Beu, S. C. 21 Tesla Fourier Transform Ion Cyclotron Resonance Mass Spectrometer: A National Resource for Ultrahigh Resolution Mass Analysis. *J Am Soc Mass Spectrom* **2015**, *26* (9), 1626-1632. DOI: 10.1007/s13361-015-1182-2 From NLM PubMed-not-MEDLINE. (45) Herzsprung, P.; Hertkorn, N.; von Tümpling, W.; Harir, M.; Friese, K.; Schmitt-Kopplin, P. Understanding
- Harir, M.; Friese, K.; Schmitt-Kopplin, P. Understanding molecular formula assignment of Fourier transform ion cyclotron resonance mass spectrometry data of natural organic matter from a chemical point of view. *Analytical and Bioanalytical Chemistry* **2014**, *406* (30), 7977-7987. DOI: 10.1007/s00216-014-8249-y.

(46) Stow, S. M.; Causon, T. J.; Zheng, X.; Kurulugama, R. T.; Mairinger, T.; May, J. C.; Rennie, E. E.; Baker, E. S.; Smith, R. D.; McLean, J. A.; et al. An Interlaboratory Evaluation of Drift Tube Ion Mobility—Mass Spectrometry Collision Cross Section Measurements. *Analytical Chemistry* **2017**, *89* (17), 9048-9055. DOI: 10.1021/acs.analchem.7b01729.

(47) Leyva, D.; Jaffé, R.; Courson, J.; Kominoski, J. S.; Tariq, M. U.; Saeed, F.; Fernandez-Lima, F. Molecular level characterization of DOM along a freshwater-to-estuarine coastal gradient in the Florida Everglades. *Aquatic Sciences* **2022**, *84* (4). DOI: 10.1007/s00027-022-00887-y.